Inorg. Chem. **2007**, *46*, 6190–6196

^{1}H Relaxivity of Water in Aqueous Suspensions of Gd^{3+}-Loaded NaY Nanozeolites and AlTUD-1 Mesoporous Material: the Influence of Si/Al Ratio and Pore Size

Małgorzata Norek,[†] Isabel C. Neves,[‡] and Joop A. Peters*,[†]

Biocatalysis and Organic Chemistry, Department of Biotechnology, Delft University of Technology, Julianalaan 136, 2628 BL Delft, The Netherlands, Departamento de Quimica, Centro de Química, Universidade do Minho Campus de Gualtar, 4710-057, Braga, Portugal

Received April 12, 2007

The results of a ^{1}H nuclear magnetic relaxation dispersion (NMRD) and EPR study on aqueous suspensions of Gd^{3+}-loaded NaY nanozeolites and AlTUD-1 mesoporous material are described. Upon increase of the Si/Al ratio from 1.7 to 4.0 in the Gd^{3+}-loaded zeolites, the relaxation rate per mM Gd^{3+} (r_1) at 40 MHz and 25 °C increases from 14 to 27 s^{-1} mM^{-1}. The NMRD and EPR data were fitted with a previously developed two-step model that considers the system as a concentrated aqueous solution of Gd^{3+} in the interior of the zeolite that is in exchange with the bulk water outside the zeolite. The results show that the observed increase in relaxivity can mainly be attributed to the residence lifetime of the water protons in the interior of the material, which decreased from 0.3 to 0.2 μs, upon the increase of the Si/Al ratio. This can be explained by the decreased interaction of water with the zeolite walls as a result of the increased hydrophobicity. The importance of the exchange rate of water between the inside and the outside of the material was further demonstrated by the relatively high relaxivity (33 s^{-1} mM^{-1} at 40 MHz, 25 °C) observed for a suspension of the Gd^{3+}-loaded mesoporous material AlTUD-1. Unfortunately, Gd^{3+} leaches rather easily from that material, but not from the Gd^{3+}-loaded NaY zeolites, which may have potential as contrast agents for magnetic resonance imaging.

Introduction

The investigation of cellular molecular events involved in normal and pathological processes by magnetic resonance imaging (MRI) is a challenging task.[1] Although MRI has a significantly higher spatial resolution (μm) than radiodiagnostic techniques (mm), its use in molecular imaging is seriously hampered by its low sensitivity. Consequently, to achieve the desired contrast enhancement, a relatively large local concentration of contrast agent (CA) is required (about 10^{-5} M)[2] as compared with other imaging modalities such as positron emission tomography, single photon emission computed tomography (10^{-11}–10^{-12} M), or optical fluorescence imaging (10^{-15}–10^{-17} M).[3]

A possible approach to overcome the problems related with the low sensitivity of MRI is to apply vectorized CAs, which would bring a high payload of paramagnetic compound to the site of interest. For lanthanide-based contrast agents, this was realized in various ways and different materials have been employed. For example, Gd^{3+}-loaded apoferritin, which allows the visualization of hepatocytes when the number of Gd cations per cell is about 4×10^7.[4] Perfluorocarbon nanoparticles containing around 94 200 Gd^{3+} ions per particle provide an extremely high relaxivity per particle and have been used successfully in molecular imaging of angiogenesis.[5–10] Gd-loaded nanoparticles consisting of Gd^{3+} bound to a core polymer that is encapsulated within a thin

* To whom correspondence should be addressed. E-mail: J.A.Peters@tudelft.nl.
[†] Delft University of Technology.
[‡] Universidade do Minho Campus de Gualtar.

(1) Weissleder, R.; Mahmood, U. *Radiology* **2001**, *219*, 316–333.
(2) Massoud, T. F.; Gambhir, S. S. *Genes Dev.* **2003**, *17*, 545–580.
(3) Weissleder, R. *Radiology* **1999**, *212*, 609–614.
(4) Aime, S.; Cabella, C.; Colombatto, S.; Crich, S. G.; Gianolio, E.; Maggioni, F. *J. Magn. Reson. Imaging* **2002**, *16*, 394–406.
(5) Yu, X.; Song, S.-K.; Chen, J.; Scott, M. J.; Fuhrhop, R. J.; Hall, C. S.; Gaffney, P. J.; Wickline, S. A.; Lanza, G. M. *Magn. Reson. Med.* **2000**, *44*, 867–872.
(6) Morawski, A. M.; Winter, P. M.; Crowder, K. C.; Caruthers, S. D.; Fuhrhop, R. W.; Scott, R. W.; Robertson, J. D.; Abendschein, D. R.; Lanza, G. M.; Wickline, S. A. *Magn. Reson. Med.* **2004**, *51*, 480–486.
(7) Winter, P.; Athey, P.; Kiefer, G.; Gulyas, G.; Frank, K.; Fuhrhop, R.; Robertson, D.; Wickline, S. A.; Lanza, G. *J. Magn. Mater.* **2005**, *293*, 540–545.

10.1021/ic700699n CCC: $37.00
Published on Web 06/23/2007

polymeric shell have been shown to provide excellent images of the gastrointestinal tract.[11]

Alternatively, this may be achieved via enhancement of T_2 relaxation times with superparamagnetic (SPM) particles, single domain ferromagnets possessing a very high magnetic moment (around 10^4 μ_B).[12,13] When iron-oxide particles are compartmentalized within cells, the internal magnetization of the compartment, due to their presence, results in large enhancements of the tranversal relaxation rate (R_2 and R_2*). Under those conditions $R_2^* \gg R_2$ and, therefore, R_2*-weighted MRI images are potentially the most sensitive to the presence of cellularly compartmentalized magnetized particles.[14−16]

For R_1-weighted images of the gastrointestinal tract, gadolinium-loaded NaY zeolites (Gd−NaY) have been developed.[17−24] Later, the synthesis of Gd^{3+}-loaded nanosized NaY zeolites opened the way for the application of this material in the imaging of the intravascular system as well. Gd^{3+} exchanged NaY nanoparticles of an average size of 80 nm, contain about 40 000 Gd^{3+} ions per particle. It has been found that the longitudinal relaxivity r_1 (r_1 is the relaxation rate expressed in s^{-1} mM^{-1} Gd^{3+}) is limited by the water exchange between the interior of zeolites and the bulk.[25] This was confirmed by the results of experiments with Gd^{3+}-loaded NaA nanozeolites,[26] which have supercages of about the same size as NaY but the access to these cages is through an eight-membered ring with diameter of only 4.1 Å as compared to 7.4 Å for zeolite NaY.[27,28]

Upon calcination of these Gd^{3+}-loaded zeolites, the lanthanide ions move irreversibly from the supercages to the small sodalite cages or their hexagonal entrance windows[29] and become less accessible for water, resulting in a decrease in relaxivity.[26] Dealumination causes the destruction of walls between cavities and by this the number of non-coordinated water molecules inside the zeolite increases, resulting in the increase of r_1 relaxivity. Surprisingly, this treatment did not influence significantly the average residence lifetime of water protons inside the cavities, which suggested that the windows of the Gd^{3+}-loaded cavities were not affected by the dealumination.[26]

Zeolites Ln-AV-9 have Ln^{3+} ions incorporated in the zeolite framework, which prohibits direct interaction between Ln^{3+} ions and water molecules. In addition these materials have small pore sizes (about 4 Å), and consequently, their r_1 relaxivity is negligible, whereas their r_2 relaxivity is high.[30] Lin et al. reported a relatively high r_1 relaxivity for a nanosized mesoporous material (Gd−MS), which had Gd^{3+} located in the framework.[31] This high relaxivity is surprising, since the Gd^{3+} ions buried in the walls of the material cannot contribute to the relaxivity to a significant extent. Most likely the high relaxivity can be attributed almost exclusively to Gd^{3+} ions immobilized by silanol groups of the pore walls. These ions are easily accessible for water molecules, which can move almost freely in and out the mesopores (pore size 20 Å). From the results of the previous studies,[25,26,30] it may be concluded that the residence lifetime of water protons inside Gd^{3+} zeolites or mesoporous materials is a major factor determining the longitudinal ^{1}H relaxivity of these materials. The Si/Al ratio in these materials determines their hydrophobicity and acidity, and therefore, it may be expected that this has an influence on the residence lifetime of water protons inside these materials and thus on their relaxivity.

In this paper we present the results of an investigation on the parameters governing the longitudinal ^{1}H relaxivities of a set of Gd^{3+}-loaded zeolite NaY nanoparticles with different Si/Al ratios. For comparison, we included a Gd^{3+}-loaded mesoporous material (Gd−AlTUD-1) in this study. The investigation is thus aimed to provide insight in the effect of the structure on the parameters governing the relaxivity. This insight may allow rational design of highly efficient r_1 contrast agents for MRI.

(8) Winter, P. M.; Caruthers, S. D.; Kassner, A.; Harris, T. D.; Chinen, L. K.; Allen, J. S.; Lacy, E. K.; Zhang, H.; Robertson, J. D.; Wickline, S. A.; Lanza, G. M. *Cancer Res.* **2003**, *63*, 5838−5843.
(9) Winter, P. M.; Morawski, A. M.; Caruthers, S. D.; Fuhrhop, R. W.; Zhang, H.; Wiliams, T. A.; Allen, J. S.; Lacy, E. K.; Robertson, J. D.; Lanza, G. M.; Wickline, S. A. *Circulation* **2003**, *108*, 2270−2274.
(10) Flacke, S.; Fisher, S.; Scott, M. J.; Fuhrhop, R.; Allen, J. S.; McLean, M.; Winter, P.; Sicard, G. A.; Gaffney, P. J.; Wickline, S. A.; Lanza, G. M. *Circulation* **2001**, *104*, 1280−1285.
(11) Reynolds, C. H.; Annan, N.; Beshah, K.; Huber, J. H.; Shaber, S. H.; Lenkinski, R. E.; Wortman, J. A. *J. Am. Chem. Soc.* **2000**, *122*, 8940−8945.
(12) Muller, R. N.; Roch, A.; Colet, J.-M.; Ouakssim, A.; Gillis, P. in Merbach, A. E.; Tóth, E.; Eds. *The Chemistry of Contrast Agents in Medical Magnetic Resonance Imaging*; John Wiley and Sons: Chichester, UK, 2001; Chapter 10.
(13) Muller, R. N.; Vander Elst, L.; Roch, A.; Peters, J. A.; Csajbók, É.; Gillis. P; Gossuin, Y. *Adv. Inorg. Chem.* **2005**, *57*, 239−292.
(14) Bowen, C. V.; Zhang, X.; Saab, G.; Gareau, P. J.; Rutt, B. K. *Magn. Reson. Med.* **2002**, *48*, 52−61.
(15) Foster-Gareau, P.; Heyn, C.; Alejski, A.; Rutt, B. K. *Magn. Reson. Med*. **2003**, *49*, 968−971.
(16) Heyn, C.; Bowen, C. V.; Rutt, B. K.; Foster, P. J. *Magn. Reson. Med*. **2005**, *53*, 312−320.
(17) Balkus, K. J., Jr.; Bresinska, I.; Kowalak, S.; Young, S. W. *Mat. Res. Symp. Proc.* **1991**, *233*, 225−230.
(18) Balkus, K. J., Jr.; Bresinska, I.; Young, S. W. *Proc. Int. Zeolite Conf.* **1992**, 193−201.
(19) Sur, S. K.; Heinsbergen, J. F.; Bryant, R. G. *J. Magn. Reson. A* **1993**, *103*, 27−33.
(20) Balkus, K. J., Jr.; Bresinska, I. *J. Alloys Comp.* **1994**, *207/208*, 25−28.
(21) Bresinska, I.; Balkus, K. J., Jr. *J. Phys. Chem*. **1994**, *98*, 12989−12994.
(22) Balkus, K. J., Jr.; Shi, J. *Microporous Mesoporous Mater*. **1997**, *11*, 325−333.
(23) Rubin, D. L.; Falk, K. L.; Sperling, M. J.; Ross, M.; Saini, S.; Rothman, B.; Shellock, F.; Zerhouni, E.; Stark, D.; Outwater, E. K.; Schmiedi, U.; Kirby, L. C.; Chezmar, J.; Coates, T.; Chang, M.; Silverman, J. M.; Rofsky, N.; Burnett, K.; Engel, J.; Young, S. W. *JMRI* **1997**, *7*, 865−872.
(24) Young, S. W.; Qing, F.; Rubin, D.; Balkus, K. J., Jr.; Engel, J.; Lang, J.; Dow, W. C.; Mutch, J. D.; Miller, R. A. *JMRI* **1995**, *5*, 499−508.
(25) Platas-Iglesias, C.; Vander Elst, L.; Zhou, W.; Muller, R. N.; Geraldes, C. F. G. C.; Maschmeyer, T.; Peters, J. A. *Chem. Eur. J.* **2002**, *8*, 5121−5131.
(26) Csajbók, É.; Bányai, I.; Vander Elst, L.; Muller, R. N.; Zhou, W.; Peters, J. A. *Chem. Eur. J.* **2005**, *11*, 4799−4807.
(27) Baerlocher, C.; Meier, W. M.; Olson, D. H. *Atlas of Zeolite Framework Types*, 5th ed., Elsevier: Amsterdam, 2001.
(28) Rakoczy, R. A.; Traa, Y. *Microporous Mesoporous Mater.* **2003**, *60*, 69−78.
(29) Klein, H.; Fuess, H.; Hunger, M. *J. Chem. Soc. Faraday Trans.* **1995**, *91*, 1813−1824.
(30) Pereira, G. A.; Ananias, D.; Rocha, J.; Amaral, V. S.; Muller, R. N.; Vander Elst, L.; Tóth, É.; Peters, J. A.; Geraldes, C. F. G. C. *J. Mater. Chem*. **2005**, *15*, 3832−3837.
(31) Lin, Y.-S.; Hung, J.; Su, J.-K.; Lee, R.; Chang, Ch.; Lin, M.-L.; Mou, Ch.-Y. *J. Phys. Chem. B* **2004**, *108*, 15608−15611.

Experimental Section

The zeolites NaY were purchased from NanoScape AG, Munich, Germany. The Al−TUD-1 material was prepared according to the procedure described in the literature.[32]

Elemental analyses were carried out with ICP-AES after dissolving the samples in a 1% HF/1.3% H_2SO_4 mixture. All samples were measured twice as an independent duplicate. The r_1 nuclear magnetic resonance dispersion (NMRD) profiles were recorded at room temperature with a field-cycling system covering a range of magnetic fields from 2.5×10^{-4} to 1.2 T (0.01−50 MHz). The relaxivities at 7 T (300 MHz) were determined with a Varian INOVA-300 spectrometer.

The EPR spectra were recorded on a Bruker ESP300E spectrometer, operating at 9.43 GHz (0.34 T, X-band) at 298 K. Typical parameters used were microwave power 4 mW, modulation amplitude 1.0 mT, and time constant 0.03 s.

Powder XRD spectra were obtained with a Philips PW1710 diffractometer using Cu Kα radiation. Both low- and wide-angle X-ray spectra were collected in order to characterize the crystallinity of the material. The textural characterization of Gd−AlTUD-1 material was based on the N_2 adsorption isotherms, determined at 77 K with a Coulter Omnisorp 100 CX apparatus. The sample was outgassed at 150 °C under vacuum prior to the measurement of the adsorption isotherm.

Room-temperature FTIR spectra were recorded on a Bomem MB104 spectrometer. The transmission spectra of the powder sample was obtained using KBr pellets over the range 4000−600 cm^{-1} by averaging 20 scans at a maximum resolution of 4 cm^{-1}.

The Gd^{3+}-loaded NaY and AlTUD-1 were prepared by stirring zeolite NaY or mesoporous AlTUD-1 in an aqueous 1 M NaCl solution at room temperature overnight. Then, the suspension was centrifuged and stirred with deionized water and centrifuged again. This procedure was repeated until the water was free of chloride ($AgNO_3$ test). The pretreated material (1 g) was suspended in deionized water (10 mL). The pH of the suspension obtained was adjusted to 5.5 with 0.1 M HCl. Then, 0.2 g of $GdCl_3 \cdot 6H_2O$ was added to the mixture and the resulting slurry was stirred overnight at room temperature.

The Gd^{3+}-loaded NaY suspensions were then dialyzed against water (cellulose tubing, Sigma, 12 KD cutoff) for 24 h, and the water was removed under reduced pressure at room temperature.

The Gd^{3+}-loaded AlTUD-1 suspension could not be dialyzed because of leaching of Gd^{3+} during the dialysis. Therefore, the material was dried at room temperature and then calcined at 550 °C in air for 12 h.

The samples for NMRD and EPR were prepared by suspending 10 mg of the solid Gd−NaY or Gd−AlTUD-1 material in doubly distilled water (10 mL) containing 0.2% of xanthan gum as a surfactant. The suspensions were dispersed in an ultrasonic bath for 5 min prior to the measurements. The relaxivities were corrected for diamagnetic contributions by subtracting relaxivities for similar suspensions of the Gd-free NaY or AlTUD-1. Relaxivies were calculated by dividing the corrected values by the Gd^{3+} concentration in the samples.

Results and Discussion

Characterization of the Gd^{3+}-Loaded Materials. The Gd^{3+}-loaded zeolites were prepared from commercially available NaY nanoparticles (particle size 70 Å) by partially exchanging the Na^+ ions for Gd^{3+}. A detailed structural analysis of Gd^{3+}-loaded NaY zeolites was performed previously.[25] The framework of zeolite Y is based on sodalite cages (which can be seen as a truncated octahedron) that are joined by oxygen bridges between the hexagonal faces. Eight sodalite cages are linked, leaving a large central cavity (supercage) with the diameter of 11.8 Å. Super-cages share a 12-membered ring with an open diameter of 7.4 Å. Because the diffusion in the small sodalite cages is very slow (1 mol in 4 days at 295 K),[33] only the Gd^{3+} ions placed in the supercages are of importance in the relaxivity process.

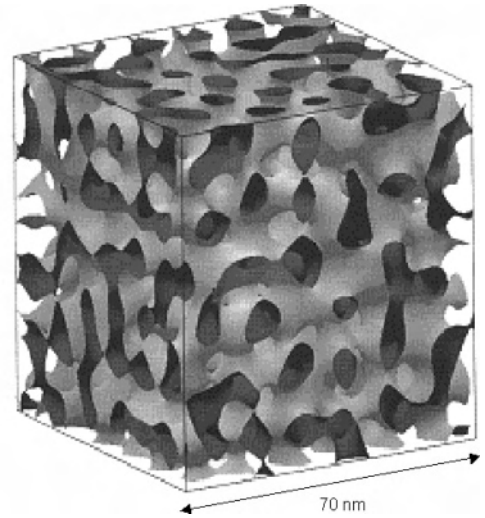

Figure 1. Computer image of spongelike mesoporous material TUD-1, comprising two endless phases of silica and pores (reproduced with permission from: Hamdy, M. S. Ph.D. thesis, Delft University of Technology, 2005).

The mesoporous material TUD-1 is characterized by well-defined pores with three-dimensional connectivities (spongelike structure, Figure 1), a high surface area, and high thermal and hydrothermal stability.[34−36] This silicate can readily be prepared with isolated metal ions, such as Al, Co, Cu, Fe, Zr, and Ti, incorporated into the surface of the pores. In this way, a negatively charged surface is obtained. The counterions (usually Na^+) can be exchanged for other cations.[37−43]

We applied Gd^{3+}-exchanged AlTUD-1 material with a Si/Al ratio of 3.5, synthesized according to a procedure

(32) Simons, C.; Hanefeld, U.; Arends, I. W. C. E.; Sheldon, R. A.; Maschmeyer, T. *Chem. Eur. J.* **2004**, *10*, 5829−5835.

(33) Basler W. D. *Ber. Bunsenges. Phys. Chem.* **1978**, *82*, 1051−1054.
(34) Jansen, J. C.; Shan, Z.; Marchese, L.; Zhou, W.; Puil, N. v. d.; Maschmeyer, T. *Chem. Commun.* **2001**, 713−714.
(35) Shan, Z.; Jansen, J. C.; Zhou, W.; Maschmeyer, T. *Appl. Catal. A: General* **2003**, *254*, 339−343.
(36) Zhang, Z.-X.; Bai, P.; Xu, B.; Yan, Z.-F. *J. Porous Mater.* **2006**, *13*, 245−250.
(37) Hamdy, M. S.; Berg, O.; Jansen, J. C.; Maschmeyer, T.; Moulijn, J. A.; Mul, G. *Chem. Eur. J.* **2006**, *12*, 620−628.
(38) Waller, P.; Shan, Z.; Marchese, L.; Tartaglione, G.; Zhou, W.; Jansen, J. C.; Maschmeyer, T. *Chem. Eur. J.* **2004**, *10*, 4970−4976.
(39) Shan, Z.; Zhou, W.; Jansen, J. C.; Yeh, C. Y.; Koegler, J. H.; Maschmeyer, T. *Stud. Surf. Sci. Catal.* **2002**, *141*, 635−640.
(40) Shan, Z.; Gianotti, E.; Jansen, J. C.; Peters, J. A.; Marchese, L.; Maschmeyer, T. *Chem. Eur. J.* **2001**, *7*, 1437−1443.
(41) Shan, Z.; Jansen, J. C.; Marchese, L.; Maschmeyer, T. *Microporous Mesoporous Mater.* **2001**, *48*, 181−187.
(42) Hamdy, M. S.; Anand, R.; Maschmeyer, T.; Hanefeld, U.; Jansen, J. C. *Chem. Eur. J.* **2006**, *12*, 1782−1789.
(43) Anand, R.; Klomp, D.; Peters, J. A.; Hanefeld, U. *J. Mol. Catal. A: Chemical* **2006**, *260*, 62−69.

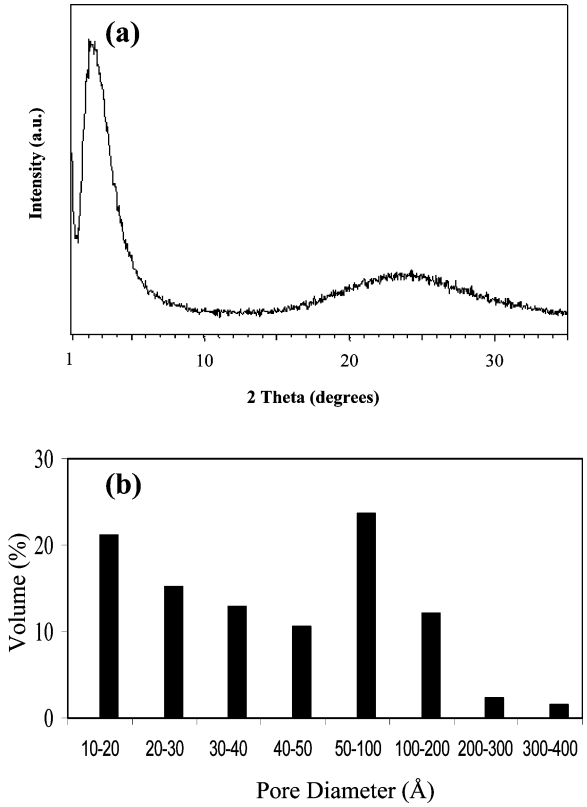

Figure 2. (a) XRD powder pattern of AlTUD-1. (b) Pore size distribution of AlTUD-1 determined by N_2 adsorption.

described elsewhere.[32] Attempts to purify the material by dialysis after the exchange with Gd^{3+} led to leaching of all Gd^{3+} present in the material. Therefore, after the ion-exchange step, the material was dried at room temperature and then calcined at 550 °C in air for 12 h. The resulting material contained 3.8% Gd.

The XRD pattern of AlTUD-1 is shown in Figure 2a. A broad peak at low angle indicates a mesoporous and amorphous character of the material. In Figure 2b the pore size distribution of AlTUD-1 is presented, as determined from N_2 adsorption. The total pore volume at $P/P_0 = 0.98$ and at 77 K was determined to be 0.409 mL/g.

The room-temperature FTIR spectra (Figure 3) of the parent and modified AlTUD-1 are dominated by the strong broad bands at 3700−3300 and 1650 cm^{-1}, which can be attributed to surface hydroxylic groups and bands corresponding to the lattice vibrations are observed in the spectral region between 1300 and 450 cm^{-1}. These bands are typical for alumina−silicate materials. No shift or broadening of these AlTUD-1 vibration bands is observed upon gadolinium loading, which indicates that the framework of AlTUD-1 remains unchanged. It can be concluded that only weak electrostatic forces are responsible for the immobilization of the Gd^{3+} ions.

Before measuring the influence of any material on the relaxivity of the water protons, it is important to check whether Gd^{3+} ions do not leach in water. It has been shown previously that Gd^{3+}-loaded zeolites NaY are stable and do not leach in aqueous suspensions at pH >2.5.[20] The stability of Gd^{3+} in mesoporous AlTUD-1 was evaluated by a xylenol

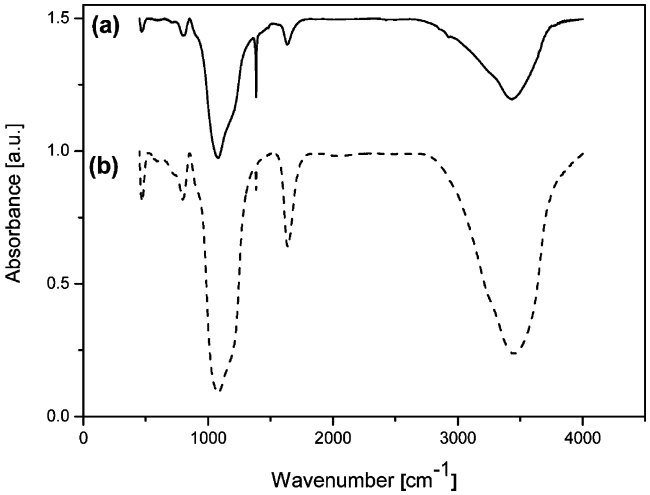

Figure 3. FT-IR spectra of AlTUD-1 (a) in comparison with Gd−AlTUD-1 (b).

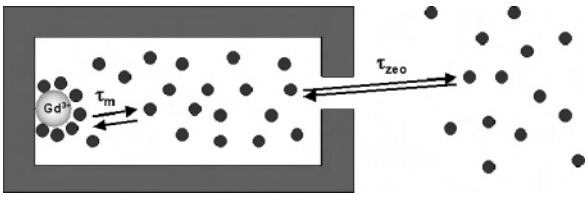

Figure 4. Schematic representation of the "two-step" model to account for the relaxivity in aqueous suspension of Gd^{3+}-loaded zeolite Y.

orange test for free Gd^{3+}.[44] When the test was performed on an aqueous suspension of Gd−AlTUD-1, it was positive. From a complexometric titration with EDTA and xylenol orange as the indicator, the amount of "free" Gd^{3+} was determined to be 4.2%, which suggests that all Gd^{3+} was extracted from the interior of the material. However, the xylenol orange test for free Gd^{3+} was negative when it was performed on the supernatant after centrifugation of a suspension of Gd−AlTUD-1. This demonstrates that, in aqueous suspensions, the Gd^{3+} is efficiently immobilized by AlTUD-1, but most likely, due to the big pore size of this material, xylenol orange and EDTA are able to enter the pores and leach out the Gd^{3+}. It may be concluded that Gd^{3+} ions in AlTUD-1 are bound relatively weakly and therefore this material is not suitable for in vivo applications. Nevertheless, we included this material in the present in vitro study, since relaxivity measurements on Gd−AlTUD-1 may provide valuable information on the influence of the pore size on the r_1 water proton relaxivity.

Relaxivity Measurements. The paramagnetic longitudinal relaxation rate enhancements of the water protons in suspension of the various materials were measured as a function of the Larmor frequency (NMRD profiles). For the zeolite Gd−NaY samples, the relaxivities (see Figure 5) appeared to be strongly dependent on the Si/Al ratios; higher relaxivities were obtained upon increasing Si/Al ratios. Upon increase of the Si/Al ratio from 1.2 to 4.0, the value of r_1 at a Larmor frequency 40 Mz increased from 14 to 27 s^{-1} mM^{-1} at 25 °C. The relaxivities of the Gd−AlTUD-1 sample were

(44) Barge, A.; Cravatto, G.; Gianolio, E.; Fedeli, F. *Contrast Med. Mol. Imaging* **2006**, *1*, 184−188.

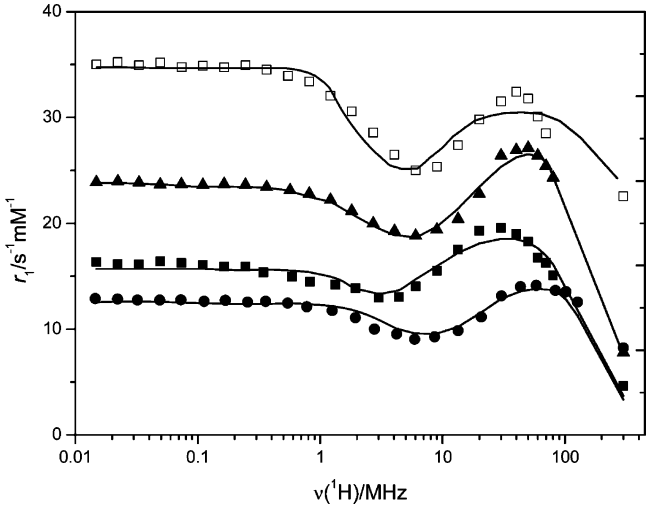

Figure 5. ^{1}H NMRD profiles of an aqueous suspension of Gd−AlTUD-1 material (empty square) and GdNaY zeolites nanoparticles with the Si/Al ratio of 4.0, 1.7, and 1.2 from top to bottom (filled symbols) at 25 °C; the suspensions always contain 0.2 wt % of xanthan.

substantially higher (33 s^{-1} mM^{-1} at 40 MHz, 25 °C) than those of the zeolitic materials. To gain insight into the parameters governing these phenomena, the data were analyzed by means of the previously developed two-step mechanism (see Figure 4).[25]

In the first step of this model, only the relaxivity inside the zeolite cavity is considered and the interior of the zeolite is treated as a concentrated solution of Gd^{3+} ions. On the basis of the model in which water protons undergo chemical exchange between two magnetically distinct environments,[45−47] eq 1 for the longitudinal relaxation rate of water protons in the interior of a zeolite was derived

$$\frac{1}{T_{1\mathrm{zeo}}} = \frac{\frac{q}{x}}{\tau_\mathrm{m} + T_{1\mathrm{m}}\left(1 + \frac{q}{x}\right)} \qquad (1)$$

in which T_{1m} is the longitudinal relaxation time of inner sphere water protons, τ_m is the mean residence lifetime of water protons in the inner sphere, q is the number of inner sphere water molecules coordinated to the Gd^{3+} ion, and x is the number of free water molecules inside the zeolite per Gd^{3+} ion. The longitudinal relaxation rate of the inner-sphere water molecules is dominated be the dipolar interaction and is given by the Solomon−Bloembergen equation:[48,49]

$$\frac{1}{T_{1\mathrm{m}}} = \frac{2}{15}\left(\frac{\mu_0}{4\pi}\right)^2 \frac{\hbar^2 \gamma_\mathrm{S}^2 \gamma_\mathrm{I}^2}{r_{\mathrm{GdH}}^6} S(S+1)\left(\frac{3\tau_{\mathrm{d}1}}{1+\omega_\mathrm{I}^2\tau_{\mathrm{d}1}^2} + \frac{7\tau_{\mathrm{d}2}}{1+\omega_\mathrm{S}^2\tau_{\mathrm{d}2}^2}\right) \qquad (2)$$

Here, r_{GdH} is the effective distance between the gadolinium electronic spin and the water protons, γ_S and γ_I are the electron and proton gyromagnetic ratios, respectively, and τ_{di} is given by $\tau_{\mathrm{di}}^{-1} = \tau_\mathrm{m}^{-1} + \tau_\mathrm{R}^{-1} + T_{\mathrm{ie}}^{-1}$ (i = 1, 2). The rotational correlation time, τ_R, concerns the rotation of the Gd^{3+}−water proton vector.

The electronic relaxation rates have been explained by the modulation of the zero field splitting (ZFS) interaction where the relaxation rates are averaged over different transitions contributing to the overall line width.[50] Later, it was shown that transverse electronic relaxation rates of some Gd^{3+} complexes, when averaged over the different relaxation times rather than over the rates, give a better description of the magnetic field dependence of the rates.[51,52] This approach resulted in eqs 3 and 4 (eq 4 is simply an empirical function; the second term should be interpreted as a special kind of spectral density function).

$$\frac{1}{T_{1\mathrm{e}}} = 1/2\Delta^2\tau_\nu[4S(S+1)-3]\left(\frac{1}{1+\omega_\mathrm{S}^2\tau_\nu^2} + \frac{4}{1+4\omega_\mathrm{S}^2\tau_\nu^2}\right) \qquad (3)$$

$$\frac{1}{T_{2\mathrm{e}}} = \Delta^2\tau_\nu\left(\frac{5.26}{1+0.372\omega_\mathrm{S}^2\tau_\nu^2} + \frac{7.18}{1+1.24\omega_\mathrm{S}\tau_\nu}\right) \qquad (4)$$

Here, ω_S is the Larmor frequency, Δ^2 is the trace of the square of the ZFS tensor, and τ_ν is the correlation time for the modulation of ZFS.

In the second step the exchange is considered of water between the inside of the zeolite and the bulk via the diffusion through the zeolite channels. This step enables the propagation of the relaxation enhancement from the interior of the material to the bulk water outside. Again assuming the chemical exchange between protons in two magnetically distinct environments, inside and outside the zeolite (this time, however, the assumption of the dilute solutions of paramagnetic species was made), eq 5 for the longitudinal relaxivity was derived.

$$r_1 = \frac{x+q}{55\,500}\left(\frac{1}{T_{1\mathrm{zeo}} + \tau_{\mathrm{zeo}}}\right) \qquad (5)$$

Here τ_{zeo} is the residence lifetime of water protons inside the zeolite.

The contribution of water molecules diffusing along the paramagnetic center without being bound to it (the outer sphere contribution[53,54]) could be neglected for both the exterior and the interior of the investigated materials because it was shown that in the case of zeolite-immobilized Gd^{3+} the contribution of this mechanism to the overall relaxivity is small, particularly at Larmor frequencies higher than 0.1 MHz.[25]

From eqs 1−5, it can be seen that the relaxivities are dependent on many variables. This makes fitting of the experimental data to these equations difficult. In order to

(45) Leigh, J. S., Jr. *J. Magn. Reson.* **1971**, *4*, 308−311.
(46) McLaughlin, A. C.; Leigh, J. S., Jr. *J. Magn. Reson.* **1973**, *9*, 296−304.
(47) Hazlewood C. F.; Chang D. C.; Nichols B. L.; Woessner D. E.; *Biophys. J.* **1974**, *14*, 583−606.
(48) Solomon, I. *Phys. Rev.* **1955**, *99*, 559−565.
(49) Bloembergen, N.; Morgan, L. O. *J. Chem. Phys.* **1961**, *34*, 842−850.
(50) McLachlan A. D. *Proc. R. Soc. London Ser. A* **1964**, *280*, 271−288.
(51) Powell, D. H.; Merbach, A. E.; González, G.; Brücher, E.; Micskei, K.; Ottaviani, M. F.; Köhler, K.; Zelewsky, A. Von; Grinberg O. Y.; Lebedev Y. S. *Helv. Chim. Acta* **1993**, *76*, 2129−2126.
(52) Powell, D. H.; Dhubhghaill, O. M. Ni; Pubanz, D.; Helm, L.; Lebedev, Y. S.; Schlaepfer, W.; Merbach, A. E. *J. Am. Chem. Soc.* **1996**, *118*, 9333−9346.
(53) Hwang, L. P.; Freed, J. H. *J. Chem. Phys.* **1975**, *63*, 4017−4025.
(54) Freed, J. H. *J. Chem. Phys.* **1978**, *68*, 4034−4037.

Table 1. Parameters Obtained from Fits of the NMRD Profiles of the Various Gd^{3+}-Loaded Materials at 25 °C[a]

	Gd−NaY		Gd−AlTUD-1	
Gd (wt %)[b]	5.7	4.9	3.7	3.8
Si/Al ratio[b]	1.2	1.7	4.0	3.5
τ_v (ps)	9 ± 2	25 ± 2	10.58 ± 0.03	48 ± 4
Δ^2 (10^{19} s^2)	6.3 ± 0.2	2.8 ± 0.1	4.2 ± 0.1	1.2 ± 0.2
τ_m (ns)	20 ± 8	14 ± 4	6.5 ± 0.6	0.27 ± 0.02
τ_{zeo} (μs)	31.5 ± 0.7	25.1 ± 0.3	20.4 ± 0.1	<10
x	17	20	26	94
q	7	7	7	3.6
ln $1/T_{2e}$ (s^{-1})	22.37	22.08	22.10	21.30
ln $1/T_{2e}$ (s^{-1})[c]	22.10	22.08	22.07	22.10

[a] Fixed parameters are underlined. [b] Si, Al, and Gd amounts in the solids as determined from ICP analysis. [c] Experimental EPR data measured at 298 K, and $B = 0.34$ T.

decrease the degrees of freedom of the system, we decided to determine independently transverse electronic relaxation rates from the linewidths in EPR spectra of the suspensions at 298 K and a magnetic field of 0.34 T (X band, 9.43 GHz). The electronic relaxation times were calculated from the line broadenings via the equation:[55]

$$\frac{1}{T_{2e}} = \frac{g_L \mu_B \pi \sqrt{3}}{h} \Delta H_{pp} \qquad (6)$$

where ΔH_{pp} is peak-to-peak EPR line widths; all other symbols have their usual meaning.

Further constraints were introduced into the fitting procedure by fixing some of the fitting parameters. Previously, we have shown that the immobilization of Gd^{3+} in zeolite NaY is so effective that the relaxivity data could be fitted with any τ_R value above 10^{-9} s, since above this limit τ_R does not affect the relaxivity anymore.[25] Therefore, the value of τ_R was fixed at 10^{-5} s. The inner-sphere Gd^{3+}−H distance was fixed at the commonly observed value of 3.1 Å. For Gd−NaY zeolite nanoparticles studied here, q was assumed to be 7 and was fixed as well in the fits. This value was dictated by EXAFS (X-ray absorption fine structure) investigations on Eu^{3+}-exchanged zeolite Y,[56] which indicate that one O atom of the framework is coordinated to Eu^{3+}, so $q = 7$ if it is assumed that the overall coordination number of Gd^{3+} is eight. Previously, we observed that the amount of water inside zeolite Gd−NaY that is in exchange with the bulk water outside is 10−12% of the weight of the zeolite, which corresponds to the amount of water present in the supercages.[25] Then, with the known amount of Gd^{3+} in the zeolites, the value of the parameter x for the various zeolites under study was calculated. These values are included in Table 1.

The best-fit parameters obtained are gathered in Table 1 and the NMRD curves obtained with these parameters are represented in Figure 5.

The best-fit values of the parameters governing the transversal electronic relaxation rates, τ_v and Δ^2, are in the range usually observed for Gd^{3+} complexes.[51] The values of $1/T_{2e}$, measured at 0.34 T, are in a good agreement with the best-fit values from the fitting procedure (see Table 1). The increase of the relaxivity observed upon an increase of the Si/Al ratio can mainly be ascribed to a decrease in both the residence lifetime of water protons in the first coordination sphere (τ_m) and the residence lifetime of water protons in the interior of the zeolite particles (τ_{zeo}). Most likely, both effects can be explained by a decrease of the interaction between water and the zeolite walls due to an increased hydrophobicity of these walls upon increasing the Si/Al ratios.[57]

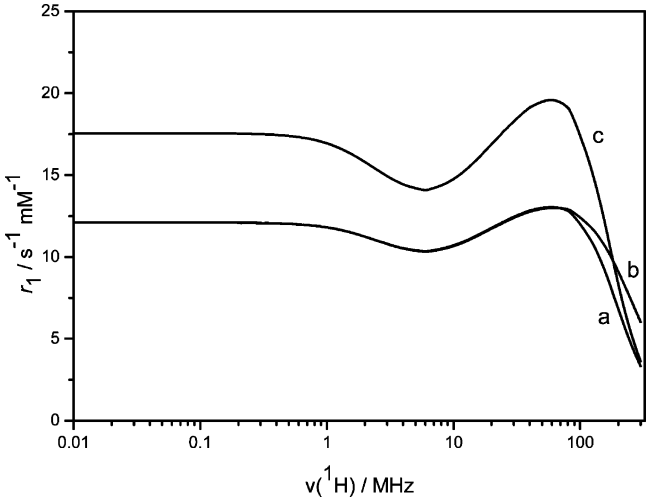

Figure 6. Simulation of the effect of the increase of τ_m and τ_{zeo}, repectively, on the NMRD profile of Gd−NaY with 5.7 wt % Gd. (a) Calculated profile for the parameters mentioned in Table 1. ($\tau_m = 20 \times 10^{-9}$ s ; $\tau_{zeo} = 3.15 \times 10^{-5}$ s). (b) Profile calculated for $\tau_m = 6.5 \times 10^{-9}$ s, while keeping all other parameters at the values used under a. (c) Profile calculated for $\tau_{zeo} = 2.04 \times 10^{-5}$ s, while keeping all other parameters at the values used under a.

Simulations show that the effect of a decrease in τ_m is small compared to that of the decrease in τ_{zeo}. Figure 6 shows as an example simulations of the effects of decreasing the values for τ_m and τ_{zeo}, respectively, while all other parameters were kept constant.

A similar fitting was performed on the data for the GdTUD-1 material. The results are included in Table 1 and Figure 5. Since q is not known in this case, q was included as an additional fitting parameter; a best-fit value of 3.6 was obtained, which suggests that about four positions are occupied due to binding to the pore walls, most likely via silanol groups. From the pore volume and the Gd^{3+} content, the value of x was calculated to be 94 mol H_2O/mol Gd. Good fits could be obtained with any value of τ_{zeo} smaller than 10 μs, showing that the diffusion of water between the inside and the outside of the Gd−AlTUD-1 material is not limiting the diffusion. The value of τ_m is an order of magnitude shorter than those for of NaY zeolites.

Conclusions

This study has demonstrated the strong influence of the hydrophobicity (Si/Al ratio) of Gd^{3+}-loaded NaY nanozeolites on the longitudinal water proton r_1 relaxivity in aqueous

(55) Reuben J.; *J. Chem. Phys.* **1971**, *75*, 3164−3167.
(56) Berry, F. J.; Carbucicchio, M.; Chiari, A.; Johnson, C.; Moore, E. A.; Mortimer, M.; Vetel, F. F. F. *J. Mater. Chem.* **2000**, *10*, 2131−2136.
(57) Verhoef, M. J.; Koster, M. J.; Poels, R. M.; Bliek, A.; Peters, J. A.; Bekkum, H. *Stud. Surf. Sci. Catal.* **2001**, *135*, 4590−4593.

suspensions. The Si/Al ratio influences mostly two parameters: the residence lifetime of water protons in the inner sphere τ_m and the residence lifetime of water protons in the interior of zeolites τ_{zeo}. With the increase of Si/Al ratio, both parameters decrease, which in turn causes an increase in the value of r_1. The effect of τ_{zeo} is relatively large compared to that of τ_m. The results with the mesoporous material Gd−AlTUD-1 demonstrate that the pore size has a dramatic effect on the efficiency of these materials on the longitudinal relaxation enhancing efficiency of this type of materials. Unfortunately, the Gd^{3+} ions in these materials are relatively weakly bound and leach out easily in the presence of chelating ligands. However, the Gd^{3+} does not leach out of the zeolitic materials, and therefore, they may have potential as contrast agents for MRI. For that application, it probably will be necessary to modify the outside surface with, for example, polyethylene glycol chains in order to avoid unspecific uptake by the reticulo endothelial system.

Acknowledgment. We thank Prof. J. C. Jansen (Delft University of Technology) for helpful discussions, Prof. F. Hagen (Delft University of Technology) for his kind help with the EPR measurements, A. Mortillaro (University of Torino, Italy) for performing NMRD measurements, and P. Pescarmona for help in the synthesis of Al−TUD-1. Thanks are due to the EU for financial support via a Marie Curie training site host fellowship (MEST-CT-2004-7442). This work was done in the frame of COST Action D38 "Metal-Based Systems for Molecular Imaging Applications" and the EU Network of Excellence European Molecular Imaging Laboratory" (EMIL, LSCH-2004-503569).

IC700699N